



# Pan evaporation paradox and evaporative demand from the past to the future over China: a review

Tingting Wang,<sup>1,2</sup> Jie Zhang,<sup>1</sup> Fubao Sun<sup>1,2,3\*</sup> and Wenbin Liu<sup>1</sup>

In a warming climate, there was a long-term expectation that the atmospheric evaporative demand would increase, which was challenged by an unexpected discovery two decades ago of decreases in measured pan evaporation, now widely termed as the ‘pan evaporation paradox.’ In this review, we summarize recent reports on the pan evaporation paradox around the world over the past half century, possible causes, implications for the water cycle, and its possible change in the future. We then present a case study of China based on the latest meteorological datasets and the state-of-the-art General Circulation Models (GCMs). We confirm that pan evaporation ( $E_{\text{pan}}$ ) decreases in most parts of China at an average of about  $-2.60 \text{ mm/y}^2$ , and this decrease disappears around 1993. We introduce and develop a detrending approach in sensitivity analysis and find that changes in solar radiation, wind speed, and relative humidity over-compensate the positive contribution of increasing air temperature in  $E_{\text{pan}}$  and lead to the well-known pan evaporation paradox. Positive changes in  $E_{\text{pan}}$  using 12 state-of-the-art GCMs for 2021–2050 and for 2071–2100 under RCP4.5 and RCP8.5 scenarios, respectively, when compared with their corresponding multi-year mean over 1971–2000 as base line, shows that the evaporation paradox would not appear in the future. We highlight that it is vital and promising to move forward to interpreting how the atmospheric evaporative demand would change in the future. © 2017 Wiley Periodicals, Inc.

How to cite this article:

*WIREs Water* 2017, e1207. doi: 10.1002/wat2.1207

## INTRODUCTION

Evaporation is the second largest component (after precipitation) of the global terrestrial water cycle, which returns about two-thirds of the average 700 mm/y of precipitation over the land.<sup>1–3</sup> Meanwhile, land evaporation consumes over half of the

total solar energy absorbed by land surfaces,<sup>4</sup> cooling the land surface.<sup>5</sup> Change in evaporation is of special concern due to its direct impact on the water–energy cycle, ecosystem stability, drought occurrence, water resources management, and human activities.<sup>1</sup> It is observed that the global mean surface temperature has increased since the late 19th century at the rate of about  $0.89^\circ\text{C}$  for 1901–2012 and about  $0.72^\circ\text{C}$  for 1951–2012.<sup>6</sup> Over decades, there was a general expectation that the hydrological cycle would be accelerated in a warming climate in a series of assessment reports by the Inter-governmental Panel on the Climate Change (IPCC)<sup>6</sup> and other research.<sup>7</sup> The expectation of changes in energy balance, which lead to both higher temperature and more energy for evaporation, should have resulted in an increase in the atmospheric evaporative demand under global warming about 30 years ago,<sup>8,9</sup> but this was

\*Correspondence to: sunfb@igsnr.ac.cn

<sup>1</sup>Key Laboratory of Water Cycle and Related Land Surface Processes, Institute of Geographic Sciences and Natural Resources Research, Chinese Academy of Sciences, Beijing, China

<sup>2</sup>College of Resources and Environment, University of Chinese Academy of Sciences, Beijing, China

<sup>3</sup>School of Civil Engineering, Hexi University, Zhangye City, Gansu Province, China

Conflict of interest: The authors have declared no conflicts of interest for this article.

challenged by an unexpected discovery of decrease in pan evaporation<sup>10</sup> from long-term observations. That discovery made by Peterson et al.<sup>10</sup> in 1995 is now widely termed as the ‘pan evaporation paradox,’<sup>11</sup> which has been observed worldwide in various sizes of evaporation pans (Figure 1).<sup>11–20</sup>

The phenomenon of the pan evaporation paradox has led to controversy among different hypotheses on the relationship between terrestrial evaporation and the evaporative demand and is highly relevant to understanding whether the global/regional hydrological cycle is accelerating<sup>11,21</sup> (Figure 1d). More scientifically, to reveal possible causes, the attribution of historical pan evaporation records to climatic forcings, for example, air temperature, net radiation/sunshine duration, wind speed, and relative humidity/vapor pressure deficit, has been undertaken.<sup>13,22–24</sup> In fact, what is overlooked is whether the evaporation paradox would appear, as well as its causes, in the future using state-of-the-art General Circulation Models (GCMs)<sup>25–30</sup> (Figure 1e). Changes in atmospheric evaporative demand have mostly been reported separately for the past and for the future, which are generally contradictory. Hence, it remains a challenge to reconcile changes of atmospheric evaporative demand in the past and for future climate.

In this review, we summarize worldwide observed evidence, possible causes, and implications for the global/regional water cycles of the pan evaporation paradox in *Review on Pan Evaporation Paradox* Section and highlight the importance of

understanding future projected change in atmospheric evaporative demand in *Evaporative Demand in GCMS* Section. We present a case study of the evaporative demand of China for the past using historical meteorological datasets and also for the future using state-of-the-art GCMs output in *A Case Study in China* Section followed by concluding remarks in last section.

## REVIEW ON PAN EVAPORATION PARADOX

### Evidence from Worldwide Observations

Starting with Peterson et al.,<sup>10</sup> the reported decline in pan evaporation over the United States and the former Soviet Union is 2–4 mm/y<sup>2</sup> from the 1950s to the early 1990s. A general declining trend throughout the Northern Hemisphere was reported at about –2 to –5 mm/y<sup>2</sup> (see Table 1, originated from Roderick et al.<sup>24</sup> and updated till now) since the 1950s<sup>11,31–34</sup> except for India and Thailand, which increased at about 10–12 mm/y<sup>2</sup>.<sup>35–37</sup> For the Southern Hemisphere, a decline rate in pan evaporation of about –3 mm/y<sup>2</sup> for 1975–2002 was first reported in Australia<sup>14</sup> and later updated to –3.2 mm/y<sup>2</sup> accounting for the installation of bird guards. New Zealand has a reported decline of –2 mm/y<sup>2</sup> since the 1970s.<sup>16</sup> The decrease in pan evaporation is almost, but not, universal; positive trends are recorded in, for instance, Spain,<sup>38</sup>

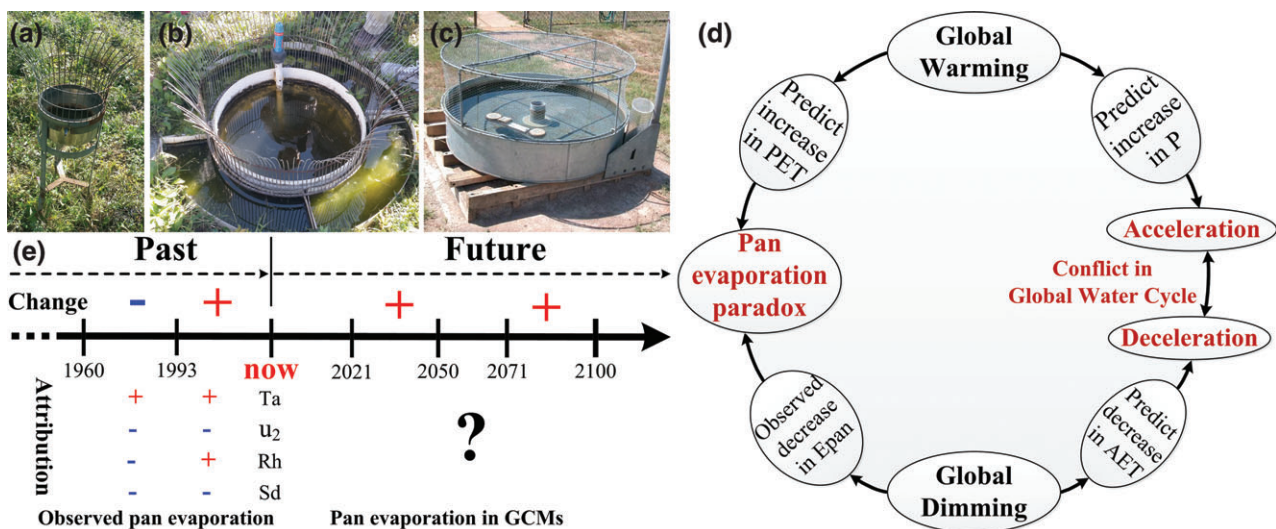


**FIGURE 1** | Evaporation pans used worldwide; (a) the D20 and (b) E601B pans used in China and (c) the Class A pan used in Australia (with bird guard) and United States (without bird guard), etc. (d) The pan evaporation paradox and its implication in global water cycle and (e) the evaporative demand from the past to the future over China, the blue ‘-’ means negative change and attribution while red ‘+’ means positive effect.

**TABLE 1** | Averaged Trends of Pan and Potential Evaporation ( $dE_{pan}/dt$  in  $mm/y^2$ ) for the Global and Regional Scales

$dE_{pan}/dt$	Region	Reference
-4	Global	Brusaert <sup>43</sup>
-3.2	Australia	Roderick and Farquhar <sup>14</sup>
-2	New Zealand	Roderick and Farquhar <sup>16</sup>
-2.2	USA	Lawrimore and Peterson <sup>44</sup>
-1.0	Canada	Burn and Hesch <sup>31</sup>
+2.94	Spain	Vicente et al. <sup>38</sup>
-3.7	Former Soviet Union	Peterson et al. <sup>10</sup> and Golubev et al. <sup>7</sup>
-12	India	Chattopadhyay and Hulme <sup>35</sup>
-1.84	Japan	Asanuma et al. <sup>45</sup>
-10.5	Thailand	Tebakari et al. <sup>36</sup>
2.24	Israel	Cohen et al. <sup>39</sup>
-24	Turkey	Ozdongan and Salvucci <sup>46</sup>
-0.93	Ireland	Black et al. <sup>32</sup>
-0.1 ~ +0.1	British Isles	Stanhill and Moller <sup>47</sup>
-0.62 <sup>1</sup>	Italy	Moonen et al. <sup>33</sup>
-5.4	China	Liu et al. <sup>48</sup>
-3.1	China (Yangtze River)	Xu et al. <sup>49</sup>
-6	China (Northwest)	Li et al. <sup>20</sup>
-4.6 (reference)	China (Tibetan Plateau)	Zhang et al. <sup>17</sup> and Brusaert <sup>19</sup>
-1.7 (potential)		
-1.1 (Pan)		
-1.2	China (Southwest)	Wang et al. <sup>50</sup>
-4.9 ~ +4.8	China (Yellow River)	Wang et al. <sup>18</sup>
-4.91 (Pan)	China (Hai River)	Zheng et al. <sup>51</sup>
-1.77 (reference)		

<sup>1</sup>Trend for 1878–2000.

Israel,<sup>39</sup> Kuwait,<sup>40</sup> part of China,<sup>41,42</sup> and part of Thailand.<sup>36</sup>

## Possible Causes of Changes in Pan Evaporation

Multiple climatic variables may contribute to changes in pan evaporation. Previous studies propose that pan evaporation changes can be partly attributed to solar radiation changes<sup>7,10,13,14,32,41,52–54</sup> and variations in aerodynamic factors, namely surface air temperature, wind speed, and relative humidity/vapor pressure deficit.<sup>15,17,31,34,50,55,56</sup> The magnitude of changes and importance of each forcing varied from region to region, as summarized in Table 2.

In attributing the changes in pan evaporation ( $E_{pan}$ ) to various meteorological variables, an important approach proposed by Roderick et al.<sup>22</sup> has been widely used. The contribution of each

variable to  $E_{pan}$  changes can be obtained by calculating the partial derivatives multiplied by annual or seasonal average trend, and the equation is as follows:

$$\frac{dE_{pan}}{dt} = \frac{\partial E_{pan}}{\partial R_n} \cdot \frac{dR_n}{dt} + \frac{\partial E_{pan}}{\partial T_a} \cdot \frac{dT_a}{dt} + \frac{\partial E_{pan}}{\partial u_2} \cdot \frac{du_2}{dt} + \frac{\partial E_{pan}}{\partial rhum} \cdot \frac{drhum}{dt} \quad (1)$$

More detailed expansion formulas of  $\frac{\partial E_{pan}}{\partial T_a}$ ,  $\frac{\partial E_{pan}}{\partial u_2}$ ,  $\frac{\partial E_{pan}}{\partial rhum}$ , and  $\frac{\partial E_{pan}}{\partial R_n}$  in Eq. (1) are provided in the literature.<sup>22,30</sup>

The model for estimating the  $E_{pan}$  is the PenPan model,<sup>57,58</sup> essentially from Penman's combination equation.<sup>23</sup> In this model, the  $E_{pan}$  in  $kg/(m^2 \cdot s)$  can be estimated as the sum of the radiative ( $E_{p,R}$ ,  $kg/(m^2 \cdot s)$ ) and aerodynamic ( $E_{p,A}$ ,  $kg/(m^2 \cdot s)$ ) components<sup>58</sup>:

**TABLE 2** | Latest Review of Attribution to Evaporation Paradox in Terms of Net Radiation/Sunshine Duration (Rn); Vapor Pressure Deficit/Relative Humidity (VPD); and Wind Speed (U) Showing Increase (+), Decrease (–), and Unchanged (–) Under the Positive Effect of Increasing Air Temperature

Region	Time	Rn	VPD	$u_2$	Region	Time	Rn	VPD	$u_2$
Australia <sup>15,22</sup>	1975–2004	–	+	–	Canada <sup>31</sup>	1971–2000	–	–	–
Former Soviet Union <sup>7,10,31</sup>	1950–1990	–	–	–	USA <sup>15</sup>	1950–2002	–	–	–
Spain <sup>38</sup>	1961–2011	~	–	–	Ireland <sup>32</sup>	1955–1984	–	–	–
India <sup>35</sup>	1940–1990	–	–	–	Thailand <sup>36</sup>	1982–2000	–	–	–
Turkey <sup>46</sup>	1979–2002	–	–	–	Israel <sup>39</sup>	1964–1998	–	+	+
China <sup>41</sup>	1955–2000	–	–	–	China <sup>48</sup>	1960–2007	–	–	–
China (Yangtze River) <sup>49</sup>	1960–2000	–	–	–	China (Yellow River) <sup>18</sup>	1957–2008	–	–	–
China (Northwest) <sup>20</sup>	1958–2010	–	–	–	China (Tibetan Plateau) <sup>17,19</sup>	1966–2003	–	–	–
						1966–2000			
China (Southwest) <sup>18,50,51</sup>	1962–2012	–	–	–	China (Hai River) <sup>51</sup>	1957–2001	–	–	–

$$E_{\text{pan}} = E_{p,R} + E_{p,A} = \left( \frac{\Delta}{\Delta + a\gamma} \frac{Rn}{\lambda} \right) + \left( \frac{a\gamma}{\Delta + a\gamma} f_q(u_2) \cdot \text{VPD} \right) \quad (2)$$

where  $\Delta$  (Pa/K) is the slope of the change in saturation vapor pressure ( $e_s$ , Pa) evaluated at a certain air temperature ( $T_a$ , K);  $\lambda$  is the latent heat of vaporization ( $2.45 \times 10^6$  J/Kg);  $a$  is the ratio of effective surface areas for vapor and heat transfer calculated based on the pan size;  $\gamma$  is the psychrometric constant ( $\approx 67$  Pa/K) that can also be calculated based on the surface air pressure above the ground (Pa); and VPD is the vapor pressure deficit (Pa) estimated using the actual vapor pressure ( $e_a$ , Pa) and the saturation vapor pressure ( $e_s$ , Pa).  $f_q(u_2)$  ( $\text{kg}/(\text{m}^2 \cdot \text{s} \cdot \text{Pa})$ ) is an empirical vapor transfer function that can be calculated using the wind speed at 2 m above the ground ( $u_2$ , m/s).

The attribution method (Eq. (1)) developed by Roderick et al.<sup>22</sup> is the key guide for separating contributions from different meteorological variables to the change in  $E_{\text{pan}}$ . The physically based PenPan model<sup>57–59</sup> (Eq. (2)) can obtain excellent agreement with measured  $E_{\text{pan}}$ , which has been tested in Australia,<sup>22,58</sup> America,<sup>15</sup> Northwest of China,<sup>20</sup> and around the world.<sup>57</sup> The decline of solar radiation<sup>13</sup> and change of aerodynamic components<sup>22</sup> like wind speed and vapor pressure deficit (or relative humidity) has offset the positive effect of increasing air temperature on the  $E_{\text{pan}}$  and led to the famous pan evaporation paradox.

## Implication on the Global Terrestrial Water Cycle

Changes in global terrestrial water cycles are difficult to predict in that there are many observations of

evaporation over terrestrial surfaces, and pan evaporation is the most widely used observed potential evaporation from adequate water supply around the world.<sup>19,22</sup> The reported decline in pan evaporation was immediately interpreted from the perspective of the global terrestrial water cycles.<sup>11,21</sup> On one hand, the decrease in pan evaporation was at first attributed to global ‘dimming’<sup>60</sup> with lower solar radiation, less evaporative demand, and thus inevitable decrease in actual evaporation and deceleration of water cycles. Therefore, the decrease in solar radiation (sunshine duration) is seen as the main cause of the decline in pan evaporation, and the widely observed decline in pan evaporation<sup>7,10,13,14,32,52</sup> is thought to be slowing down the global terrestrial hydrological cycle, which is then expected to speed up as global dimming moves to brightening.<sup>60</sup> A complementary theory on terrestrial evaporation and pan evaporation expects that increased terrestrial evaporation, that is, an accelerated global hydrological cycle, would increase moisture in the air, thus reducing pan evaporation. This complementary hypothesis is formulated by Brutsaert and Parlange<sup>11</sup> and supported by Lawrimore and Peterson<sup>44</sup> and Golubev et al.<sup>7</sup> This hypothesis suggests that the soil water content, terrestrial evaporation, and the effect of their interaction on variation in aerodynamic components, for example, the decline in wind speed<sup>15,17,22,31,61</sup> and change in vapor pressure deficit or relative humidity,<sup>15,34,35,37,38,50</sup> play major roles in the evaporation paradox. In bringing the two perspectives together of whether the water cycle is accelerating or decelerating, Roderick and Farquhar,<sup>62</sup> Sun et al.,<sup>63</sup> and Yang et al.<sup>21</sup> proposed to use the Budyko curve to explain the regional hydrological cycle based on pan evaporation and precipitation, which provides an ecohydrological perspective on the pan evaporation paradox.

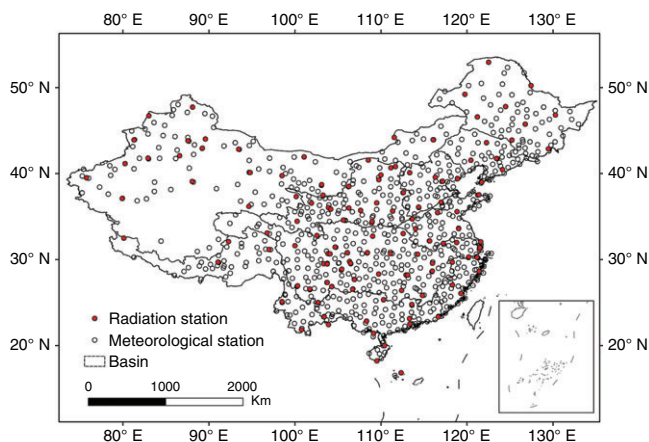


**FIGURE 2** | Distribution of radiation and meteorological stations over China.

## EVAPORATIVE DEMAND IN GCMs

Previous research on the pan evaporation paradox mainly focused on observations of historical periods. In fact, the very first study explicitly projecting higher evaporative demand in a warmer climate was by Rind et al.<sup>8,9</sup> using climate models. How will evaporative demand change in the future as a consequence of the ongoing accumulation of greenhouse gases in the atmosphere? How can we incorporate recent advances in the pan evaporation paradox study into projecting future evaporative demand?

GCMs are currently the most widely used sources in assessing and projecting potential evaporation,<sup>25,58,64,65</sup> and the PenPan model has been well used in estimating pan evaporation using GCMs outputs.<sup>30</sup> Feng and Fu<sup>26</sup> pointed out that

potential evaporation would increase over terrestrial surface almost everywhere at about 230 mm/y in the RCP8.5 scenario in the 21st century, and other studies reported increases at global and regional scale.<sup>27,29,66</sup> Furthermore, it is not conclusively established that the evaporative demand would increase under an enhanced greenhouse climate.<sup>25</sup> The CO<sub>2</sub>-induced increase in temperature alone would no doubt have a positive effect on potential evaporation.<sup>26,27</sup> However, some studies have highlighted the lack of temperature-based estimations of potential evaporation in climate change assessments,<sup>67–69</sup> and physically based potential evaporation calculation are more robust. Underlying reasons, like the change of net radiation,<sup>13</sup> slight decrease in wind speed,<sup>24</sup> and increase in vapor pressure deficit,<sup>27,70</sup> have likely contributed to the future change of evaporative demand. Very recently, Liu and Sun<sup>30,71</sup> assessed the ability of 12 GCMs in estimating pan evaporation and projected an increasing evaporative demand in the future over China.

## A CASE STUDY IN CHINA

The decline of potential evaporation trend has been well reported in China<sup>41,63</sup> as well as at the regional scale, such as for the Tibetan Plateau,<sup>17,19,72</sup> the Yangtze River Basin,<sup>49</sup> the Yellow River Basin,<sup>18</sup> the Hai River Basin,<sup>51</sup> Northwest China,<sup>20</sup> and Southwest China,<sup>50</sup> while potential evaporation increased in some parts.<sup>41</sup> Here, we use pan evaporation in China as a case study to interpret the pan evaporation paradox in the past and the projection for the future using state-of-the-art climate models.

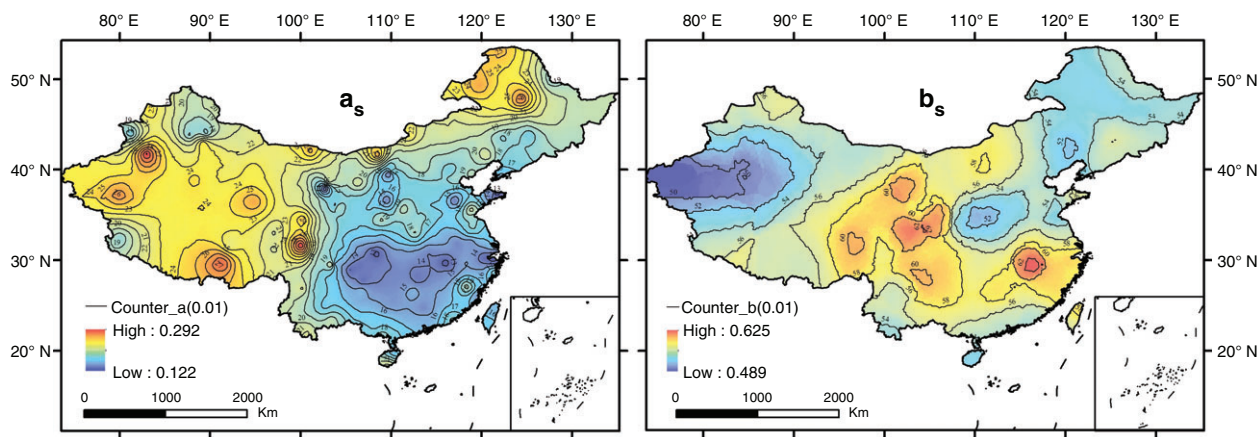


**FIGURE 3** | The newly adjusted parameters of  $a_s$  and  $b_s$  used to estimate the net radiation from the sunshine duration (the actual value shall be the value in each counter line multiplied by 0.01).

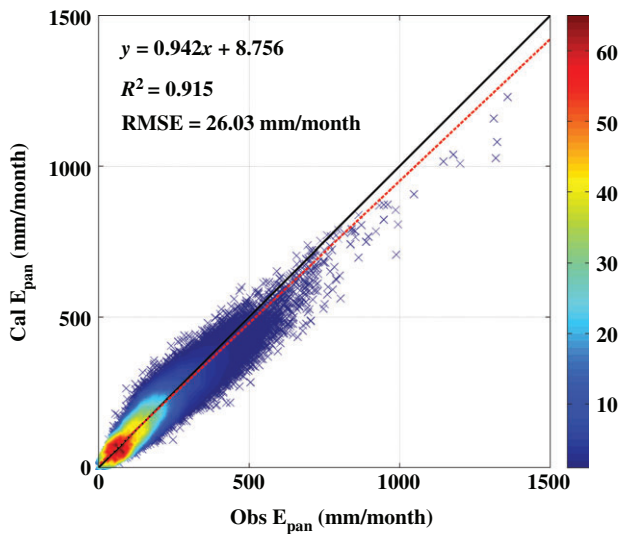


**FIGURE 4** | Correlation of observed pan evaporation (Obs  $E_{pan}$ ) and calculated evaporation using the PenPan model (Cal  $E_{pan}$ ) (327230 pairs of monthly observed pan and calculated  $E_{pan}$  plotted, and the color bar is the density of value within an interval of 61.05 mm/month).

### Observed Pan Evaporation in China

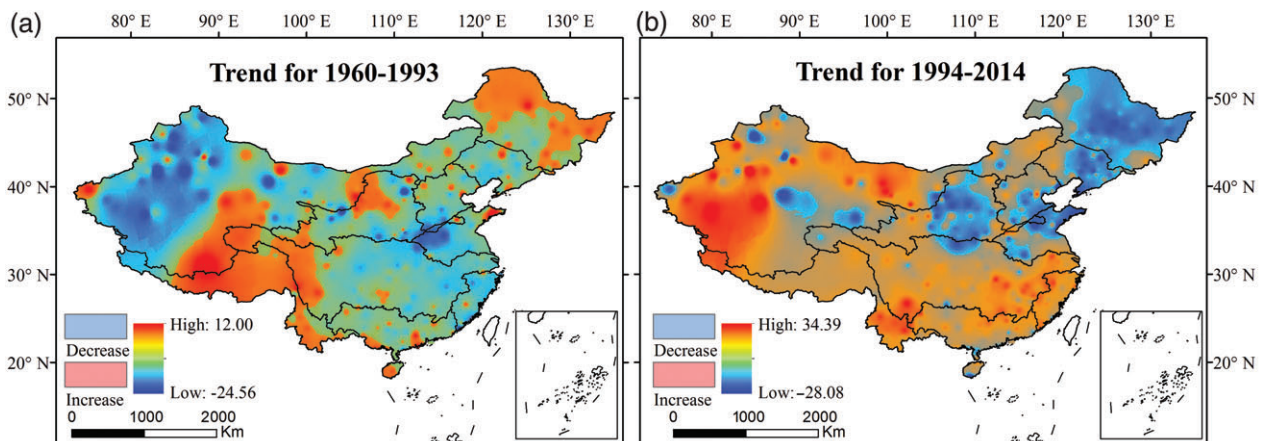
We adopt the physically based PenPan model<sup>22,57–59</sup> (Eq. (2)) to estimate pan evaporation (the diameter of the pan is 20 cm, hereafter D20). From there, we estimate the D20 pan evaporation using the latest datasets collected from the meteorological stations distributed across China (Figure 2). The parameters  $a_s$  and  $b_s$  in the Angstrom formula<sup>73</sup> are adjusted (Figure 3) using data from radiation stations (red dots in Figure 2), and good agreement between observed and calculated  $E_{pan}$  is achieved (see

Figure 4). As shown in Figure 3, the adjusted parameter  $a_s$  varies from place to place with a range of 0.12–0.29 and  $b_s$  of 0.450–0.63, which would effectively improve the estimated FAO-Penman<sup>73</sup> results of generally suggested values of 0.25 and 0.50 and in turn affect the radiative component of  $E_{pan}$  and thus the final estimation. Instead of the commonly used empirical wind speed function developed by Thom,<sup>59</sup> we calibrate the wind function as,

$$f_q(u_2) = 3.977 \times 10^{-8}(1 + 0.505u_2) \quad (3)$$

which applied to the whole of China, so as to adjust the systematic bias of the simulated  $E_{pan}$  for the D20 pan. After the calibration of the solar radiation estimation, we obtain a good agreement between observed and calculated  $E_{pan}$  with an  $R^2$  of 0.92 and RMSE of 26.03 mm/month (Figure 4).

The annual change of  $E_{pan}$  over China for the most recent period of 1960–2014 and the forcings are shown in Figure 5, and the spatial pattern of the periodical trends are shown in Figure 6. The annual  $E_{pan}$  exhibits an obvious downward trend for 1960–1993 at about  $-2.60 \text{ mm/y}^2$  and then reverses upward from 1994 at  $4.29 \text{ mm/y}^2$  over China (Figure 5), showing strong evidence of the evaporation paradox for the period of 1960–1993, generally in line with worldwide observations.<sup>11,33,34,41,50</sup> For the recent period of 1994–2014, the strong warming period, the  $E_{pan}$  starts to go up. The relative humidity (rh<sub>um</sub>) remains almost unchanged for 1960–1993 but decreases at about  $-0.17\%$  for 1994–2014, while the sunshine duration (Sd) decreases during the first period but stays almost unchanged for the latter period. The change of the wind speed ( $u_2$ ) (termed



**FIGURE 5** | The distribution of pan evaporation trends of China for two periods with the positive trend covered with a mask of red and negative with blue, respectively: (a) the trend for the period 1960–1993 of  $-24.56 \sim +12.00 \text{ mm/y}^2$  and (b) trend for 1994–2014 with range of  $-28.08 \sim +34.39 \text{ mm/y}^2$ .

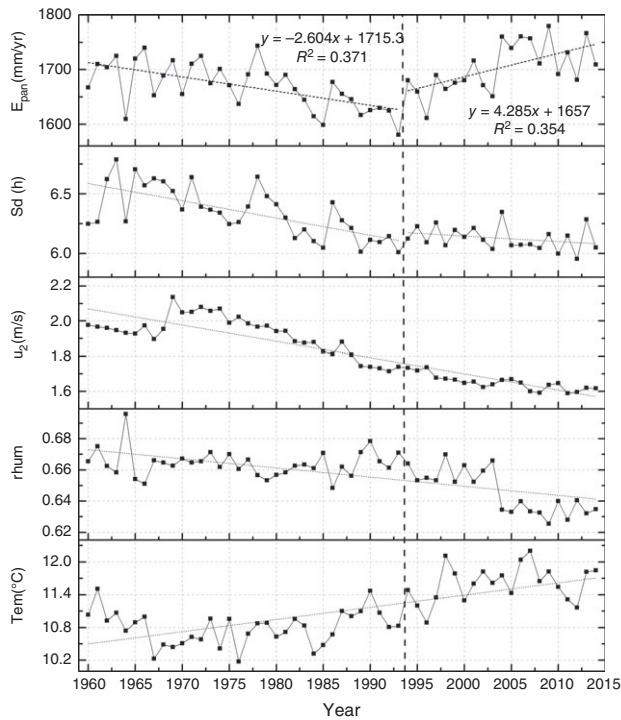


**FIGURE 6** | Pan evaporation changes as well as annual time series of the sunshine duration (Sd), the wind speed ( $u_2$ ), the relative humidity (rhum), and the air temperature (Tem) in China for 1960–2014.

‘global stilling’<sup>22,61</sup>), Sd, and rhum (Figure 4) can lead to a decrease in  $E_{pan}$ , while the continuous increasing of air temperature (T) is no doubt likely to increase the  $E_{pan}$ . These four meteorological forcings work interactively and change  $E_{pan}$  to varying degrees. About 77.4% of the area of China shows a downward trend, except for part of the Tibet Plateau and several other small parts, for 1960–1993 (Figure 6). For 1994–2013, about 69.1% of the area shows an increasing trend, and the evaporation paradox disappears in most parts of China.

**TABLE 3** | The Statistical Information (Mean, RMSE, and Bias) of the Calculated Rate of Change Based on Annual Time Series of  $E_{pan}$  ( $T_{Epan}$ ); the Attributing Results Based on the Detrending Approach (Detrend) and PD Method (PD) for 1960–1993 and 1994–2014, Respectively

	Y1960–1993 (mm/y <sup>2</sup> )			Y1994–2014 (mm/y <sup>2</sup> )		
	Mean	RMSE	Bias	Mean	RMSE	Bias
$T_{Epan}$	–2.91			2.56		
Detrend	–2.59	2.06	–0.93	1.68	2.11	–1.02
PD	–2.40	3.81	1.83	0.86	3.76	–1.86

### Causes of Changes of Pan Evaporation in the Past

Currently, the attribution method (Eq. (1)) proposed by Roderick et al.,<sup>22</sup> the partial differentiation (PD) method, has been widely used. To make a comparison, in this study, we apply a detrending approach, which originates in signal capture research and is later used in drought monitoring,<sup>69</sup> hydrology, climate change,<sup>74</sup> etc. It helps eliminate the long-term trends in original meteorological forcings so as to separate the role of climate trends and variability. Zhang et al.<sup>69</sup> first used this detrending approach to quantify the contribution of each forcing to PDSI. Here, we use the detrending approach proposed by Zhang et al.<sup>69</sup> in the sensitivity analysis of pan evaporation and make simple comparisons with the commonly used PD method first.

We summarize the comparison regarding the attributing results based on the PD method and the detrending approach against the calculated rate of change using the annual time series of  $E_{pan}$  (labeled  $T_{Epan}$  in Table 3) of selected stations. The results in Table 3 show that the detrending approach is superior to the traditional PD method in attributing changes of  $E_{pan}$  to the mean value closer to the calculated rate of change of  $E_{pan}$  for the periods of 1960–1993 and 1994–2014. The RMSE and Bias estimated based on the detrending approach are 2.06 mm/y<sup>2</sup> and –0.93 mm/y<sup>2</sup>, respectively, in comparison with 3.81 mm/y<sup>2</sup> and 1.83 mm/y<sup>2</sup> using the PD method for 1960–1993, indicating a better estimation using the detrending approach in attributing change of the  $E_{pan}$ . The same conclusion holds for 1994–2014. The spatial distributions of the contribution of each forcing are shown in Figure 7.

For the period of 1960–1993, the rapid decrease of wind speed ( $u_2$ ) of about 0.01 m/s leads to a –2.56 mm/y<sup>2</sup> change in  $E_{pan}$ , which accounts for about 60% of the averaged change in  $E_{pan}$  and is mostly a negative trend, except in the southwest part of China where a positive effect is detected. The solar duration (Sd) comes next, leading to about –0.95 mm/y<sup>2</sup> in  $E_{pan}$  and an air temperature of +0.92 mm/y<sup>2</sup>. So, the decreasing  $u_2$  is the main reason why the pan evaporation paradox and the negative effect due to decreasing sunshine duration almost neutralizes the positive effect of increasing air temperature.

For 1994–2013, the wind speed, air temperature (Tem), and relative humidity (rhum) affect the  $E_{pan}$ , which on average attributes about –1.41 mm/y<sup>2</sup>, +1.12 mm/y<sup>2</sup> and +2.68 mm/y<sup>2</sup>, respectively, while a small reduction of sunshine duration attributes much less. Large variability between the

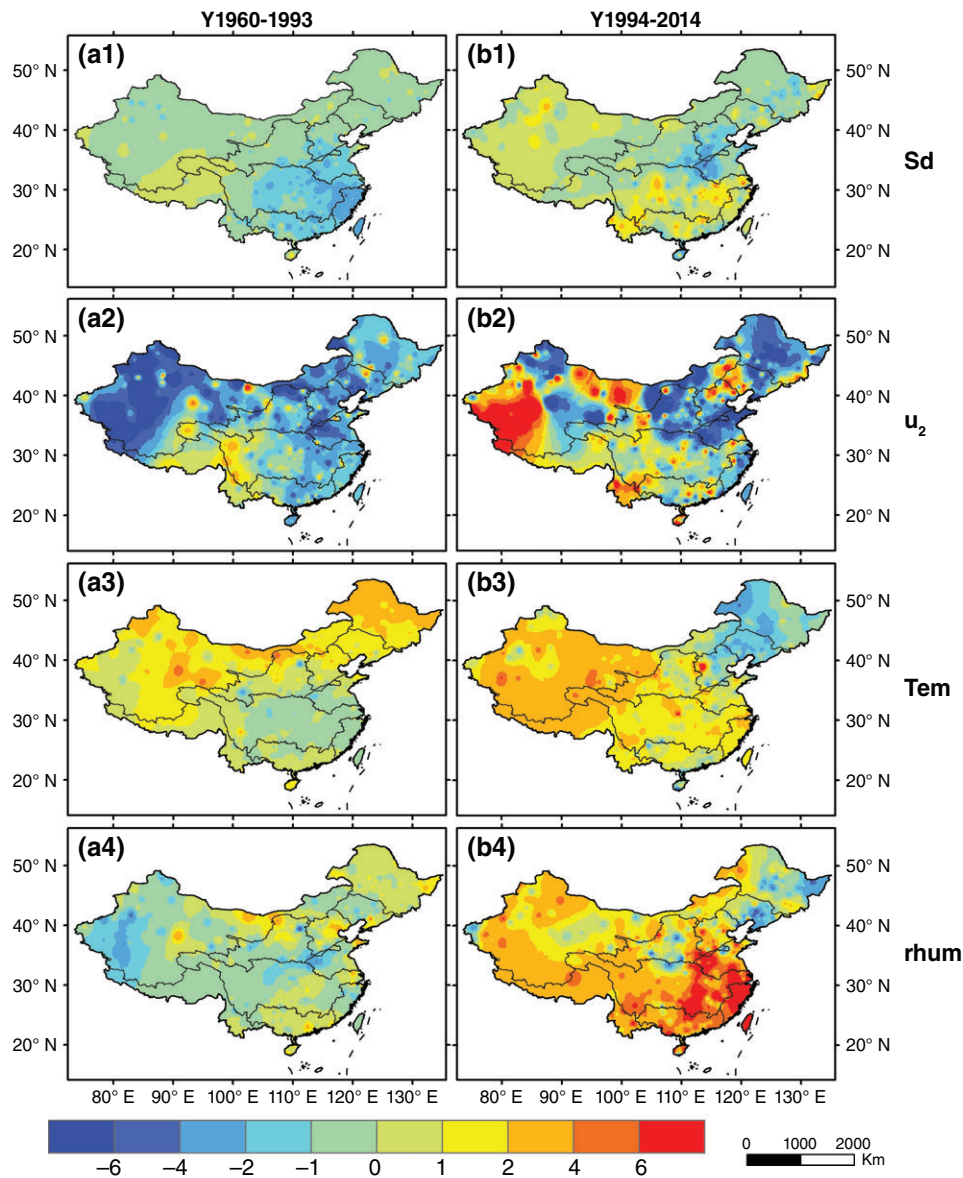


**FIGURE 7** | Sensitivity analysis of pan evaporation for 1960–1993 (left column) and 1994–2014 (right column): (a1) the contribution of  $S_d$  for 1960–1993 and (b1) for 1994–2014, (a2) the contribution of  $u_2$  for 1960–1993 and (b2) for 1994–2014, (a3) the contribution of  $Tem$  for 1960–1993 and (b3) for 1994–2014, (a4) the contribution of  $rh_{um}$  for 1960–1993 and (b4) for 1994–2014.

maximum increase in the west and decrease in the northeast is due to the effect of wind speed. The rise of air temperature leads to about a  $4\text{--}6\text{ mm/y}^2$  increase in pan evaporation around China, except in the northeast, and a greater than  $4\text{ mm/y}^2$  increase due to the change of relative humidity in almost the whole of China.

### Projected Change in Evaporative Demand in the Future

We use 12 state-of-the-art Coupled Model Intercomparison Project Phase 5 (CMIP5) GCMs<sup>30</sup> to access

and project the future evaporative demand for China. First, we calculate the multiyear mean  $E_{pan}$  anomalies (the mean value of whole China as the base line) for 1961–2000 (D20 pan evaporation data available for this period), and the results are shown in Figure 8. All the GCMs underestimate the observed  $E_{pan}$  to some degree, but the spatial pattern of most GCMs resembles the observations in different parts of China, for example, the MRI model well captures the anomaly in the northeast, north, and part of southwest, and the CNRM model best represents the change in northwest, although none can fully match the whole of China. None of the

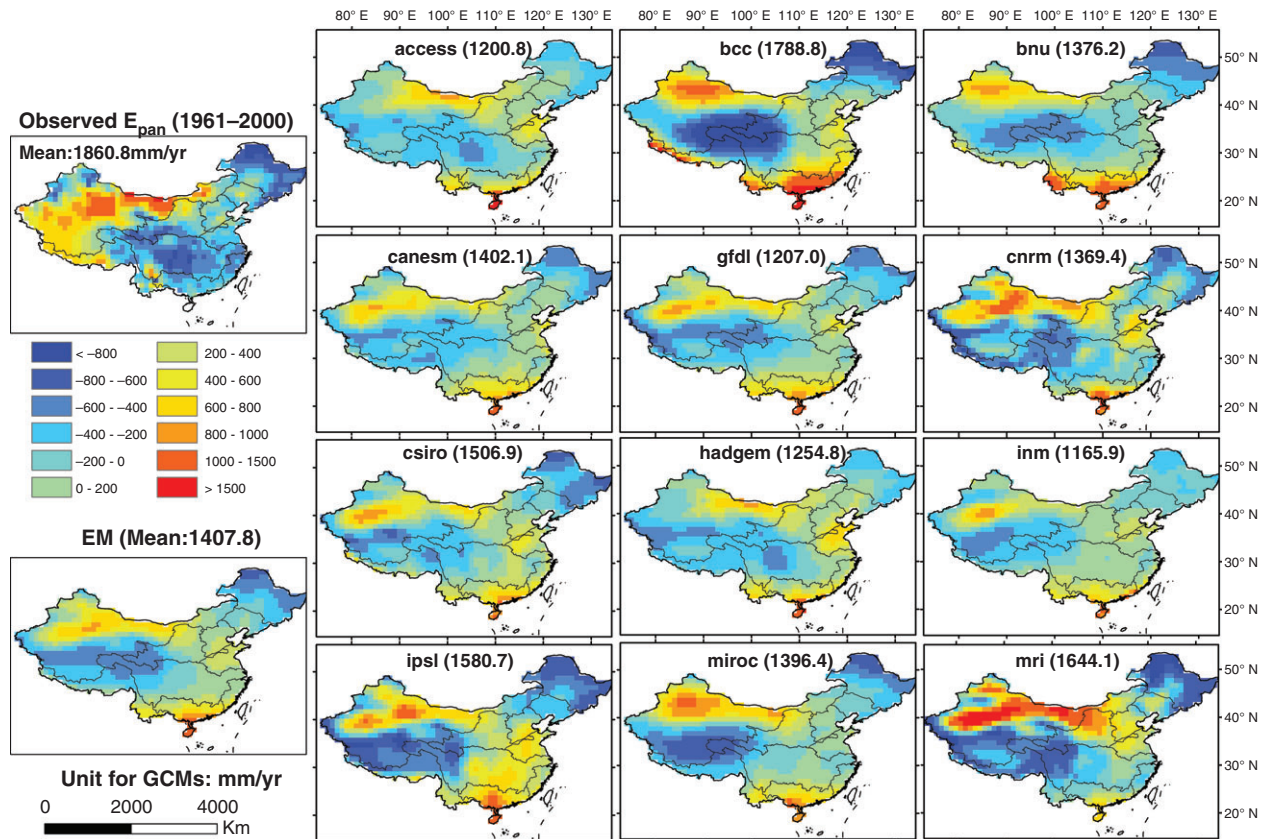


**FIGURE 8** | Comparison of mean annual observed pan evaporation and calculated  $E_{pan}$  of 12 GCMs as well as their ensemble mean (EM) (anomalies for 1961–2001) over China; the value in the brackets is the overall mean in the unit of mm/yr of each GCM.

calculated  $E_{pan}$  resembles the observed  $E_{pan}$  in the Tibetan Plateau probably because the meteorological and pan evaporation data are relatively limited in such a complicated topography.

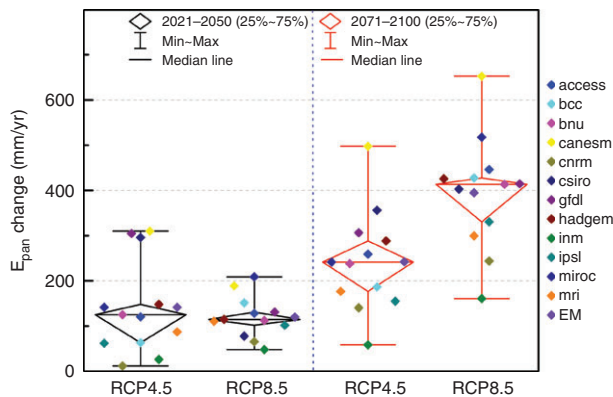


**FIGURE 9** | Changes of mean annual pan evaporation in 12 GCMs and their ensemble mean (EM) over China for 2021–2050 (black box and dots) and 2071–2100 (red box and dots, the HADGEM GCM ends in 2099) under RCP4.5 and RCP8.5 scenarios, respectively, in comparison with the control period of 1971–2000.

The CMIP5 climate models under two emission scenarios (Representative Concentration Pathway, RCP 4.5 and RCP 8.5) are used to project future changes of  $E_{pan}$  over China in order to provide insight into changes of water and energy cycles and water resources and agricultural water management in a warming climate. After bias correction,<sup>30</sup> the future simulations (2021–2050 and 2071–2100) under RCP4.5 and RCP8.5 scenarios are then calculated. The historical multiyear averaged  $E_{pan}$  (1971–2000) in each GCM are used as base line to project the  $E_{pan}$  change. The spatial deficits of multiyear averaged  $E_{pan}$  between future cases and base line are shown in Figure 9. The GCMs results project changes of 141.5 mm/y (11.9–310.1 mm/y) and 120.1 mm/y (47.9–208.6 mm/y) in multiyear averaged  $E_{pan}$  for 2021–2050 and 242.1 mm/y (58.7–498.0 mm/y) and 394.7 mm/y (161–652.7 mm/y) for 2071–2100, under both low (RCP4.5) and high (RCP8.5) scenarios, respectively. The INM and HADGEM models overestimate the  $E_{pan}$  under the RCP4.5 scenario and thus the mean value of 12 GCMs compared with the RCP8.5 scenario.

## CONCLUDING SUMMARY

In this review, we summarized recent reports on the pan evaporation paradox around the world over the past half century, possible causes, and its possible changes in the future. Changes in pan evaporation have mostly been reported separately for the past and for the future. It remains a challenge to reconcile changes of atmospheric evaporative demand in the past and for the future. We used China as a case study to understand changes in atmospheric evaporative demand from the past to the future based on meteorological data and state-of-the-art climate models. We confirmed that the pan evaporation decreases in most parts of China on an average of about  $-2.60 \text{ mm/y}^2$ , known as 'evaporation paradox,' and disappears around 1993, which is consistent with Sun et al.<sup>63</sup> We proposed a calibrated wind function ( $f_q(u_2) = 3.977 \times 10^{-8}(1 + 0.505u_2)$ ) for the PenPan model in simulating the specific D20 pan evaporation with good performance. We introduced a detrending approach to attribute changes in pan evaporation, which performs better than the commonly used partial differentiation method. Changes in solar radiation, wind speed, and

vapor pressure deficit offset the positive contribution of air temperature in  $E_{\text{pan}}$  and lead to the well-known pan evaporation paradox. Using the latest observations for 1994–2014, the warming signal is strong enough, together with the decrease in relative humidity neutralizing the negative attribution of wind speed in some regions, leading to strengthening evaporative demand. Furthermore, all the 12 GCMs underestimated the observed  $E_{\text{pan}}$  but with reasonable spatial pattern in most GCMs. After applying a bias correction technique, the GCMs project multiyear averaged changes of  $141.5 \text{ mm/y}$  (11.9–310.1 mm/y) and  $120.1 \text{ mm/y}$  (47.9–208.6 mm/y) for 2021–2050 and  $242.1 \text{ mm/y}$  (58.7–498.0 mm/y) and  $394.7 \text{ mm/y}$  (161–652.7 mm/y) for the 2071–2100 under RCP4.5 and RCP8.5 scenarios, respectively, when compared with the multiyear averaged  $E_{\text{pan}}$  over the base line period (1971–2000).

By comprehensively reviewing literature on the pan evaporation paradox over last two decades and presenting a case study over China, we show that it is vital to interpret how atmospheric evaporative demand will change in the future.

## ACKNOWLEDGMENTS

This study was financially supported by the National Key Research and Development Program of China (2016YFA0602402 and 2016YFC0401401), the CAS Pioneer Hundred Talents Program (Dr. Fubao Sun), and the Open Research Fund of State Key Laboratory of Desert and Oasis Ecology in Xinjiang Institute of Ecology and Geography, Chinese Academy of Sciences (CAS).

## REFERENCES

- Chahine MT. The hydrological cycle and its influence on climate. *Nature* 1992, 359:373–380.
- Oki T, Kanae S. Global hydrological cycles and world water resources. *Science* 2006, 313:1068–1072.
- Allen MR, Ingram WJ. Constraints on future changes in climate and the hydrologic cycle. *Nature* 2002, 419:224–232.
- Trenberth KE, Fasullo JT, Kiehl J. Earth's global energy budget. *Bull Am Meteorol Soc* 2009, 90:311–323.
- Shukla S, Safeeq M, AghaKouchak A, Guan K, Funk C. Temperature impacts on the water year 2014 drought in California. *Geophys Res Lett* 2015, 42:4384–4393.
- IPCC. *Climate Change 2013: The Physical Science Basis: Working Group I Contribution to the Fifth Assessment Report of the Intergovernmental Panel on Climate Change*. Cambridge, U. K.: Cambridge University Press; 2014.
- Golubev VS, Lawrimore JH, Groisman PY, Speranskaya NA, Zhuravin SA, Menne MJ, Peterson TC, Malone RW. Evaporation changes over the contiguous United States and the former USSR: a reassessment. *Geophys Res Lett* 2001, 28:2665–2668.
- Rind D. The doubled CO<sub>2</sub> climate and the sensitivity of the modeled hydrologic cycle. *J Geophys Res Atmos* 1988, 93:5385–5412.
- Rind D, Goldberg R, Hansen J, Rosenzweig C, Ruedy R. Potential evapotranspiration and the likelihood of future drought. *J Geophys Res Atmos* 1990, 95:9983–10004.
- Peterson T. Evaporation losing its strength. *Nature* 1995, 377:687–688.
- Brutsaert W, Parlange M. Hydrologic cycle explains the evaporation paradox. *Nature* 1998, 396:30–30.

12. Zhang Y, Peña-Arancibia JL, McVicar TR, Chiew FH, Vaze J, Liu C, Lu X, Zheng H, Wang Y, Liu YY. Multi-decadal trends in global terrestrial evapotranspiration and its components. *Sci Rep* 2016, 6:1–7.
13. Roderick ML, Farquhar GD. The cause of decreased pan evaporation over the past 50 years. *Science* 2002, 298:1410–1411.
14. Roderick ML, Farquhar GD. Changes in Australian pan evaporation from 1970 to 2002. *Int J Climatol* 2004, 24:1077–1090.
15. Hobbins MT, Ramírez JA, Brown TC. Trends in pan evaporation and actual evapotranspiration across the conterminous US: paradoxical or complementary? *Geophys Res Lett* 2004, 31:405–407.
16. Roderick ML, Farquhar GD. Changes in New Zealand pan evaporation since the 1970s. *Int J Climatol* 2005, 25:2031–2039.
17. Zhang Y, Liu C, Tang Y, Yang Y. Trends in pan evaporation and reference and actual evapotranspiration across the Tibetan Plateau. *J Geophys Res Atmos (1984–2012)* 2007, 112:1103–1118.
18. Wang W, Shao Q, Peng S, Xing W, Yang T, Luo Y, Yong B, Xu J. Reference evapotranspiration change and the causes across the Yellow River Basin during 1957–2008 and their spatial and seasonal differences. *Water Resour Res* 2012, 48:113–122.
19. Brutsaert W. Use of pan evaporation to estimate terrestrial evaporation trends: the case of the Tibetan Plateau. *Water Resour Res* 2013, 49:3054–3058.
20. Li Z, Chen Y, Shen Y, Liu Y, Zhang S. Analysis of changing pan evaporation in the arid region of Northwest China. *Water Resour Res* 2013, 49:2205–2212.
21. Yang D, Sun F, Liu Z, Cong Z, Lei Z. Interpreting the complementary relationship in non-humid environments based on the Budyko and Penman hypotheses. *Geophys Res Lett* 2006, 33:122–140.
22. Roderick ML, Rotstajn LD, Farquhar GD, Hobbins MT. On the attribution of changing pan evaporation. *Geophys Res Lett* 2007, 34:251–270.
23. Roderick ML, Hobbins MT, Farquhar GD. Pan evaporation trends and the terrestrial water balance. II. Energy balance and interpretation. *Geogr Compass* 2009, 3:761–780.
24. Roderick ML, Hobbins MT, Farquhar GD. Pan evaporation trends and the terrestrial water balance. I. Principles and observations. *Geogr Compass* 2009, 3:746–760.
25. Wild M, Ohmura A, Cubasch U. GCM-simulated surface energy fluxes in climate change experiments. *J Clim* 1997, 10:3093–3110.
26. Feng S, Fu Q. Expansion of global drylands under a warming climate. *Atmos Chem Phys* 2013, 13:081–100.
27. Fu Q, Feng S. Responses of terrestrial aridity to global warming. *J Geophys Res Atmos* 2014, 119:7863–7875.
28. Prudhomme C, Williamson J. Derivation of RCM-driven potential evapotranspiration for hydrological climate change impact analysis in Great Britain: a comparison of methods and associated uncertainty in future projections. *Hydrol Earth Syst Sci* 2013, 17:1365–1377.
29. Yin Y, Ma D, Wu S, Pan T. Projections of aridity and its regional variability over China in the mid-21st century. *Int J Climatol* 2015, 35:4387–4398.
30. Liu W, Sun F. Assessing estimates of evaporative demand in climate models using observed pan evaporation over China. *J Geophys Res Atmos* 2016, 121:8329–8349.
31. Burn DH, Hesch NM. Trends in evaporation for the Canadian Prairies. *J Hydrol* 2007, 336:61–73.
32. Black K, Davis P, Lynch P, Jones M, McGettigan M, Osborne B. Long-term trends in solar irradiance in Ireland and their potential effects on gross primary productivity. *Agric For Meteorol* 2006, 141:118–132.
33. Moonen A, Ercoli L, Mariotti M, Masoni A. Climate change in Italy indicated by agrometeorological indices over 122 years. *Agric For Meteorol* 2002, 111:13–27.
34. Jung M, Reichstein M, Ciais P, Seneviratne SI, Sheffield J, Goulden ML, Bonan G, Cescatti A, Chen J, De Jeu R. Recent decline in the global land evapotranspiration trend due to limited moisture supply. *Nature* 2010, 467:951–954.
35. Chattopadhyay N, Hulme M. Evaporation and potential evapotranspiration in India under conditions of recent and future climate change. *Agric For Meteorol* 1997, 87:55–73.
36. Tebakari T, Yoshitani J. *Swanpimol C*. Journal of Hydrologic Engineering: Time-space trend analysis in pan evaporation over Kingdom of Thailand; 2005.
37. Bandyopadhyay A, Bhadra A, Raghuvanshi N, Singh R. Temporal trends in estimates of reference evapotranspiration over India. *J Hydrol Eng* 2009, 14:508–515.
38. Vicente-Serrano SM, Azorin-Molina C, Sanchez-Lorenzo A, Revuelto J, Morán-Tejeda E, López-Moreno JL, Espejo F. Sensitivity of reference evapotranspiration to changes in meteorological parameters in Spain (1961–2011). *Water Resour Res* 2014, 50:8458–8480.
39. Cohen S, Ianetz A, Stanhill G. Evaporative climate changes at Bet Dagan, Israel, 1964–1998. *Agric For Meteorol* 2002, 111:83–91.
40. Salam MA, Mazrooei SA. Changing patterns of climate in Kuwait. *Asian J Water Environ Pollut* 2007, 4:119–124.
41. Liu B, Xu M, Henderson M, Gong W. A spatial analysis of pan evaporation trends in China, 1955–2000.

- J Geophys Res Atmos* 1984–2012 2004, 109: 1255–1263.
42. Han S, Xu D, Wang S. Decreasing potential evaporation trends in China from 1956 to 2005: accelerated in regions with significant agricultural influence? *Agric For Meteorol* 2012, 154:44–56.
  43. Brutsaert W. Indications of increasing land surface evaporation during the second half of the 20th century. *Geophys Res Lett* 2006, 33:382–385.
  44. Lawrimore JH, Peterson TC. Pan evaporation trends in dry and humid regions of the United States. *J Hydrometeorol* 2000, 1:543–546.
  45. Asanuma J, Kamimera H. Long-term trend of pan evaporation measurements in Japan and its relevance to the variability of the hydrological cycle. In: *Symposium on water resource and its variability in Asia in the 21st century*, March; 2004.
  46. Ozdogan M, Salvucci GD. Irrigation-induced changes in potential evapotranspiration in southeastern Turkey: test and application of Bouchet's complementary hypothesis. *Water Resour Res* 2004, 40:W04301.
  47. Stanhill G, Möller M. Evaporative climate change in the British Isles. *Int J Climatol* 2008, 28:1127–1137.
  48. Liu X, Luo Y, Zhang D, Zhang M, Liu C. Recent changes in pan-evaporation dynamics in China. *Geophys Res Lett* 2011, 38:142–154.
  49. Xu C, Gong L, Jiang T, Chen D, Singh V. Analysis of spatial distribution and temporal trend of reference evapotranspiration and pan evaporation in Changjiang (Yangtze River) catchment. *J Hydrol* 2006, 327:81–93.
  50. Wang J, Wang Q, Zhao Y, Li H, Zhai J, Shang Y. Temporal and spatial characteristics of pan evaporation trends and their attribution to meteorological drivers in the Three-River Source Region, China. *J Geophys Res Atmos* 2015, 120:6391–6408.
  51. Zheng H, Liu X, Liu C, Dai X, Zhu R. Assessing contributions to panevaporation trends in Haihe River Basin, China. *J Geophys Res Atmos* 2009, 114:144–153.
  52. Jhajharia D, Shrivastava S, Sarkar D, Sarkar S. Temporal characteristics of pan evaporation trends under the humid conditions of northeast India. *Agric For Meteorol* 2009, 149:763–770.
  53. Ji Y, Zhou G. Important factors governing the incompatible trends of annual pan evaporation: evidence from a small scale region. *Clim Change* 2011, 106:303–314.
  54. Fu G, Charles SP, Yu J. A critical overview of pan evaporation trends over the last 50 years. *Clim Change* 2009, 97:193–214.
  55. Tanaka N, Kume T, Yoshifuji N, Tanaka K, Takizawa H, Shiraki K, Tantasirin C, Tangtham N, Suzuki M. A review of evapotranspiration estimates from tropical forests in Thailand and adjacent regions. *Agric For Meteorol* 2008, 148:807–819.
  56. van Heerwaarden CC, Vilà-Guerau de Arellano J, Teuling AJ. Land-atmosphere coupling explains the link between pan evaporation and actual evapotranspiration trends in a changing climate. *Geophys Res Lett* 2010, 37.
  57. Linacre ET. Estimating U.S. class A pan evaporation from few climate data. *Water Int* 1994, 19:5–14.
  58. Rotstayn LD, Roderick ML, Farquhar GD. A simple pan-evaporation model for analysis of climate simulations: evaluation over Australia. *Geophys Res Lett* 2006, 33:254–269.
  59. Thom A, Thony JL, Vauclin M. On the proper employment of evaporation pans and atmometers in estimating potential transpiration. *Q J Roy Meteorol Soc* 1981, 107:711–736.
  60. Wild M. Global dimming and brightening: a review. *J Geophys Res Atmos* 1984–2012 2009, 114:D00D16.
  61. McVicar TR, Van Niel TG, Li LT, Roderick ML, Rayner DP, Ricciardulli L, Donohue RJ. Wind speed climatology and trends for Australia, 1975–2006: capturing the stilling phenomenon and comparison with near-surface reanalysis output. *Geophys Res Lett* 2008, 35.
  62. Roderick ML, Sun F, Lim WH, Farquhar GD. A general framework for understanding the response of the water cycle to global warming over land and ocean. *Hydrol Earth Syst Sci* 2014, 18: 1575–1589.
  63. Sun F, Yang D, Liu Z, Cong Z. Study on coupled water-energy balance in Yellow River basin based on Budyko Hypothesis. *J Hydraul Eng* 2007, 38:409–416.
  64. Lawrence DM, Thornton PE, Oleson KW, Bonan GB. The partitioning of evapotranspiration into transpiration, soil evaporation, and canopy evaporation in a GCM: impacts on land atmosphere interaction. *J Hydrometeorol* 2007, 8:862.
  65. Noilhan J, Lacarrère P. GCM grid-scale evaporation from mesoscale modeling. *J Clim* 1995, 8:206–223.
  66. Lin L, Gettelman A, Fu Q, Xu Y. Simulated differences in 21st century aridity due to different scenarios of greenhouse gases and aerosols. *Clim Change* 2016:1–16.
  67. Hobbins MT, Dai A, Roderick ML, Farquhar GD. Revisiting the parameterization of potential evaporation as a driver of long-term water balance trends. *Geophys Res Lett* 2008, 35:150–152.
  68. Milly P, Dunne KA. On the hydrologic adjustment of climate-model projections: the potential pitfall of potential evapotranspiration. *Earth Interact* 2011, 15:1–14.

69. Zhang J, Sun F, Xu J, Chen Y, Sang Y, Liu C. Dependence of trends in and sensitivity of drought over China (1961–2013) on potential evaporation model. *Geophys Res Lett* 2016, 43:206–213.
70. Scheff J, Frierson DM. Scaling potential evapotranspiration with greenhouse warming. *J Clim* 2014, 27:1539–1558.
71. Liu W, Sun F. projecting and attributing future changes of evaporation demand over China in CMIP5 climate models. *J. Hydrometeor.* doi:10.1175/JHM-D-16-0204.1.
72. Zhang Y, Chiew FH. Relative merits of different methods for runoff predictions in ungauged catchments. *Water Resour Res* 2009, 45:4542–4548.
73. Allen RG, Pereira LS, Raes D, Smith M. Crop evapotranspiration - guidelines for computing crop water requirements - FAO Irrigation and drainage paper 56. FAO 1998, 56:15–79.
74. Mao Y, Nijssen B, Lettenmaier DP. Is climate change implicated in the 2013–2014 California drought? A hydrologic perspective. *Geophys Res Lett* 2015, 42:2805–2813.